Ultra High Molecular Weight Polyethylene/Organoclay Hybrid Nanocomposites

Eon M. Lee,[1] Young S. Oh,[2] Ha S. Ha,[3] Ham M. Jeong,[4] Byung K. Kim[1]

[1]*Department of Polymer Science and Engineering, Pusan National University, Busan 609-735, Korea*
[2]*Kolon Central Research Park, Kolon Industries, Inc., Goomi, Gyungbuk 730-030, Korea*
[3]*R&D Center, Korea Petrochemical Ind. Co., Ltd., Ulsan 680-110, Korea*
[4]*Department of Chemistry, University of Ulsan, Ulsan 680-741, Korea*

Received 9 January 2009; accepted 18 April 2009
DOI 10.1002/app.30736
Published online 23 June 2009 in Wiley InterScience (www.interscience.wiley.com).

ABSTRACT: The ultra high molecular weight polyethylene (UHMWPE)/organoclay nanocomposites were prepared in decalin with various organoclay contents (0, 1, 2, 3, and 5 pphr). Transmission electron micrographic images and X-ray diffraction results showed that the organoclay was exfoliated and well dispersed in UHMWPE matrix. The rheological properties were measured at various temperatures (110, 130, and 150°C) in a broad range of shear rate (10^{-1}–10^{2}) at a gel concentration of 6 wt %. The result showed that the viscosity increased with the addition and increasing organoclay content. Thermal stability (thermogravimetric analysis) and crystallinity (differential scanning calorimeter) of UHMWPE increased with increasing organoclay content implying that the organoclay functioned as barrier and nucleating agent. © 2009 Wiley Periodicals, Inc. J Appl Polym Sci 114: 1529–1534, 2009

Key words: Organoclay; nanocomposites; PE

INTRODUCTION

Ultra-high molecular weight polyethylene (UHMWPE) offers superior mechanical properties and chemical resistance based on its high molecular weight.[1–3] Consequently, it has been used in a number of specific areas including bearing components, gears, sporting goods, guide rails, and medical materials in total joint replacement.[4–7]

Nanocomposites are promising materials for applications where improved mechanical properties, thermal stability, and chemical resistance are desired.[8] Because nanofillers such as carbon nanotubes, nanoclays, and nanofibres can be used at lower concentrations than conventional fillers, processability is facilitated in nanocomposites.[9,10]

However, it is difficult to prepare UHMWPE/nanofillers composites using conventional melt mixing technology due to the high viscosity of UHMWPE. Therefore, solvent and compatibilizer have been used to facilitate processing.[11]

It has been reported that the addition of UHMWPE to electrically conducting composite can eliminate the positive temperature coefficient effect and improves the reproductivity of electrical conductivity. The positive temperature coefficient effect is a phenomenon of sharp resistivity increase when the temperature approaches the melting point in an electrically polymer conducting composite consisting insulator polymer and conductive carbon black or carbon fiber.[12] Silver nanoparticles were also introduced into the UHMWPE by supercritical fluid processing. The presence of silver nanoparticles resulted in enhanced wear resistance and tribological properties, implying that supercritical fluid procedure can decrease the process of polymer/metal tribolo-chemical debris formation and enhance UHMWPE biocompatibility and antimicrobial activity.[13]

In this study, the UHMWPE/organoclay nanocomposites were prepared in decalin with various organoclay contents (0, 1, 2, 3, and 5 pphr) in the presence of a compatibilizer (Polyethylene-*g*-maleic anhydride copolymer (PE-*g*-MAH)) at a resin concentration of 6 wt %. Rheological, thermal, mechanical properties, and morphology of the nanocomposites have been measured.

EXPERIMENTAL

Materials and preparation

The organoclay (Cloisite® 15A) used in this study is obtained from Southern Clay Products (Gonzales, TX). PE-*g*-MAH (Aldrich, MAH ~ 3 wt %) was used as a compatibilizer, whereas UHMWPE of $M_W = 4.5 \times 10^6$ g/mol was used. The resin (UHMWPE(9)/PE-*g*-MAH(1)) concentration in decalin was fixed at 6% and organoclay contents were 1, 2, 3, and 5 pphr, respectively (Table I). Organoclay was first added to decalin,

Correspondence to: B. K. Kim (bkkim@pnu.edu).
Contract grant sponsors: PNU-IFAM JRC and Medium term Strategy Technology Development Program from Ministry of Knowledge and Economy.

Journal of Applied Polymer Science, Vol. 114, 1529–1534 (2009)

TABLE I
Basic Formulation to Prepare UHMWPE/Organoclay Composites ((UHMWPE + PE-*g*-MAH)/Decalin = 96/4)

RUN#	UHMWPE	PE-*g*-MAH	Cloisite 15A (phr)	Decalin
		6		
1	100	0	0	
2	90	10	1	
3	90	10	2	94
4	90	10	3	
5	90	10	5	

followed by ultrasonification for 3 h. To this, PE-*g*-MAH was added and completely dissolved at 135°C. Subsequently, the UHMWPE powder was added to the solutions and stirred until the powder was completely dissolved to form clear solution. Finally, sample was put in an oven and dried to obtain the nanocomposites.

X-ray diffraction profiles

X-ray diffraction (XRD) patterns were recorded with symmetric reflection mode by using Rigaku (Tokyo, Japan) X-ray diffractometer (30 kV, 25 mA). A monochromatic CuKα radiation was used. For each scanning interval of 2°/min, diffracted X-ray intensity was automatically recorded.

Tensile properties

The tensile properties of the nanocomposites were measured with a universal testing machine (Lloyd Instruments) at a crosshead of 500 mm/min using specimens prepared according to ASTM D-1822. Tests were made at room temperature and at least three runs were made to report the average.

Thermal properties

Thermogravimetric analysis (TGA) has been done using TGA Q50 (TA Instruments, New Castle, DE). A 6–8 mg of sample was put in an alumina crucible and heated to 600°C at 10°C/min under N_2 atmosphere, where the flow rate of N_2 was 60–40 mL/min.

Thermal properties of the UHMWPE/organoclay nanocomposites were determined using a differential scanning calorimeter (DSC, Dupont 1000, Twin Lakes, WI). Samples were heated to 200°C to erase the thermal history of the sample and cooled to 30°C at 5°C/min recording crystallization behavior. Melting endotherm was recorded during the second heating cycle at 10°C/min.

Rheological properties

The rheological behavior of the composites was measured using an Advaned Rheological Extension System (Rheometric Scientific, Piscataway, NJ) in a parallel plate geometry with diameter of 25 mm and gap of 1 mm. Strain sweep was first done at 110°C and 10 rad/s to identify the linear viscoelastic limit. Frequency sweeps were measured at three different temperatures (110, 130, and 150°C) from 0.1 to 100 rad/s at 12% strain, which is the upper limit of linear viscoelastic behavior of our resins at the measure temperatures.

RESULTS AND DISCUSSION

XRD profiles

Figure 1 shows XRD profiles of virgin organoclay (Cloisite®15A) and UHMWPE/organoclay nanocomposites, where the organoclay contents were 1, 2, 3, and 5 pphr, respectively.

The diffraction peak at $2\theta = 2.75^\circ$ gives the interlayer spacing (d-spacing) of 32.09 Å for the original Cloisite®15A, which was calculated by Bragg's law [eq. (1)].

$$n\lambda = 2d \sin\theta \quad (1)$$

No peak was observed for 1, 2, and 3 pphr organoclay, implying that the layers of clay have been well exfoliated. But peak appears for 5 pphr organoclay content at lower diffraction angles, viz. at $2\theta = 1.21^\circ$ corresponding to d-spacing of 72.92 Å. This indicates that organoclays are intercalated but not well exfoliated by PE-*g*-MAH and ultrasonication.

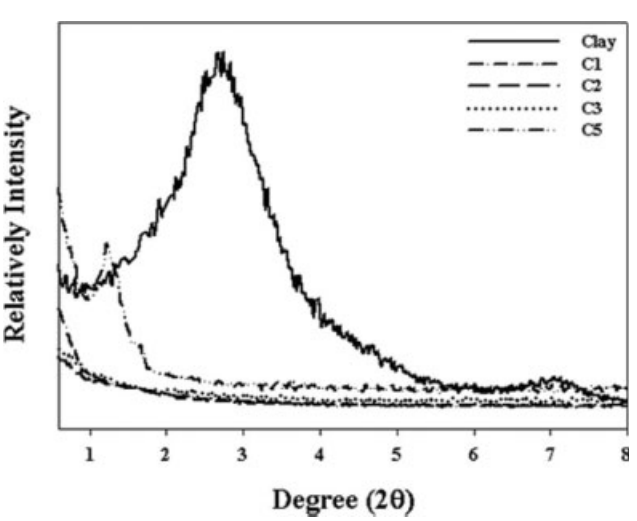

Figure 1 XRD patterns of UHMWPE/organoclay nanocomposites.

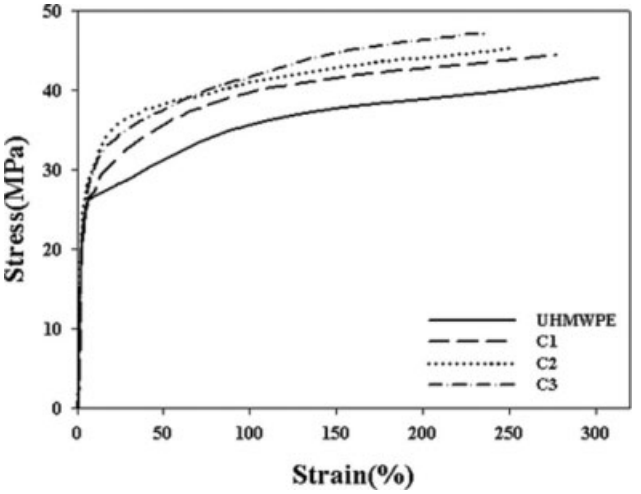

Figure 2 Stess–strain behaviors of UHMWPE/organoclay nanocomposites.

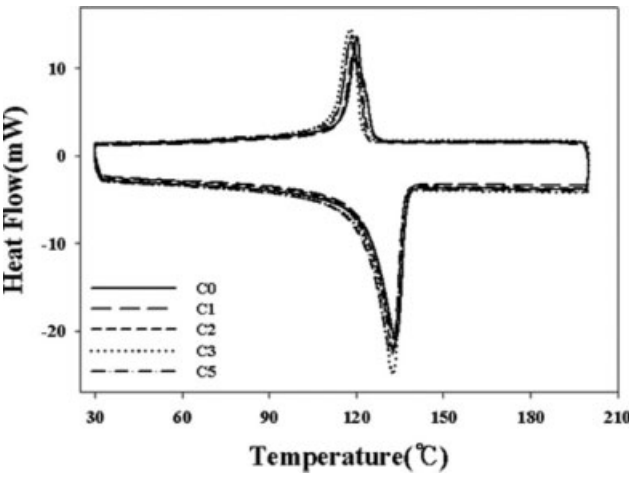

Figure 4 DSC thermogram of UHMWPE and UHMWPE/organoclay nanocomposites.

Mechanical properties

Tensile properties of UHMWPE/organoclay nanocomposite are shown in Figure 2. The stress–strain curves for all samples are similar. UHMWPE does not show yield, and modulus smoothly decreases until the fracture at about 300% elongation. The tensile modulus and strength generally increase and elongation at break decreases with the addition and increasing amount of organoclay as compared with the virgin UHMWPE. However, the tensile strength decreases for 5 pphr organoclay due to its incomplete exfoliation along with aggregations. Similar results have also been reported in other articles.[14–17]

Thermal properties

TGA measurements (Fig. 3) show that thermal resistance is enhanced in the presence of nanoclay due to the thermal insulation effect of clay.[18,19]

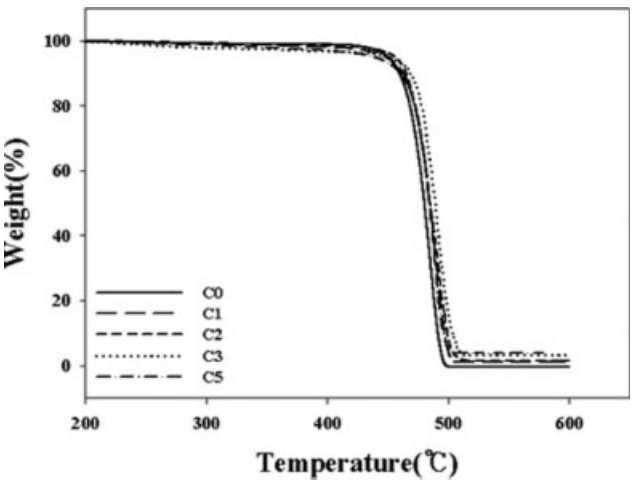

Figure 3 TGA curves of UHMWPE/organoclay nanocomposites.

DSC thermograms of the nanocomposites as well as UHMWPE are shown in Figure 4 along with the detailed date in Table II. It is seen that crystalline melting temperature (T_m) of UHMWPE (132.7°C) is slightly decreased in nanocomposites. As expected, the melting enthalpy and crystallinity (X_c) increases in nanocomposites, implying that organoclay provides the UHMWPE with nucleating agent. It is also noted that the increase is small with C5 as described earlier. It is mentioned that crystallinity of the sample was calculated using the heat of fusion for crystalline PE (7.87 kJ/mol or 281.1 J/g).

Rheological properties

Figures 5 and 6 show the shear-dependent complex (η^*), dynamic (η'), and elastic part (η'') of viscosities for various compositions of UHMWPE/organoclay composites at various temperatures (110, 130, and 150°C). It is seen that the composite viscosity increases with increasing organoclay content. Dispersion viscosity can be described by a power law as:

$$\eta_{rel} = 1 + k_1\Phi + k_2\Phi^2 + \cdots \quad (2)$$

where ks are constants, Φ is the volume fraction of dispersed phase, viz. clay. Below the crystallization temperature, the crystalline volume of the UHMWPE should also contribute to the dispersed phase. The viscosity functions generally follow the power law behavior [eq. (3)] within the experimental

TABLE II
DSC Data of UHMWPE/Organoclay Composites (X_c = % Crystallinity, ΔH = Heat of Fusion)

	Clay	C1	C2	C3	C5
2θ (°)	2.75	–	–	–	1.21
d-spacing(Å)	32.09	Exfoliated	Exfoliated	Exfoliated	72.92

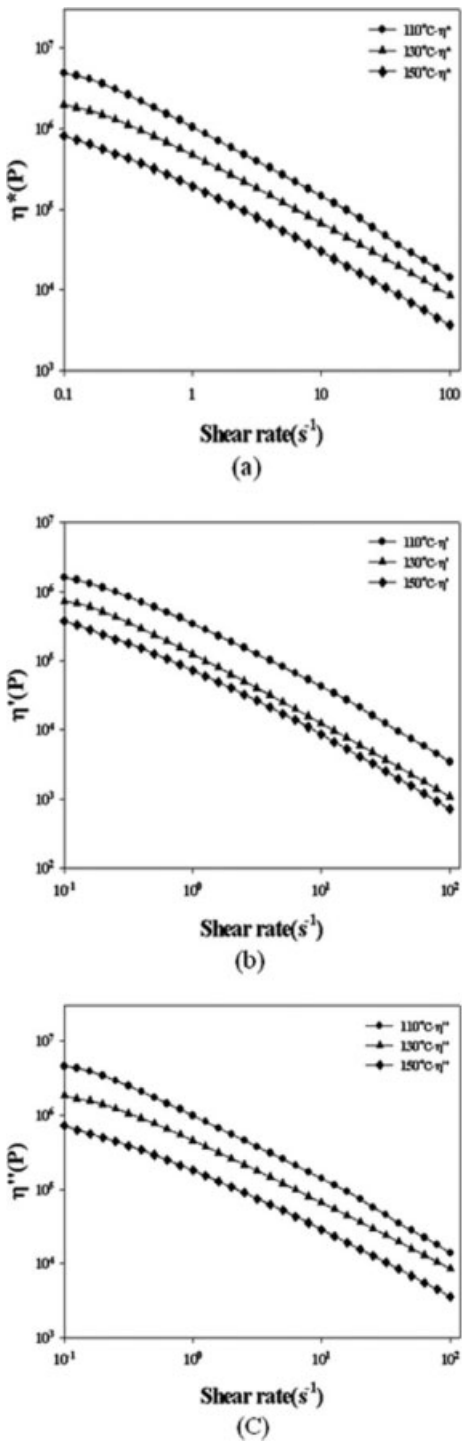

Figure 5 Shear viscosity of UHMWPE/organoclay (1 pphr) nanocomposites at various temperatures: (a) complex viscosity, η^*, (b) dynamic viscosity, η', and (c) dynamic out-of-phase viscosity, η''.

ranges of temperature and composite composition.

$$\eta = m \times \dot{\gamma}^n \tag{3}$$

where η is the viscosity, m is a constant, and n is power-law index.

The dynamic viscosity corresponds to the viscous deformation of the material, whereas the loss part of the complex viscosity is the fluid elasticity.

$$\eta^* = \eta' - i\eta'' \tag{4}$$

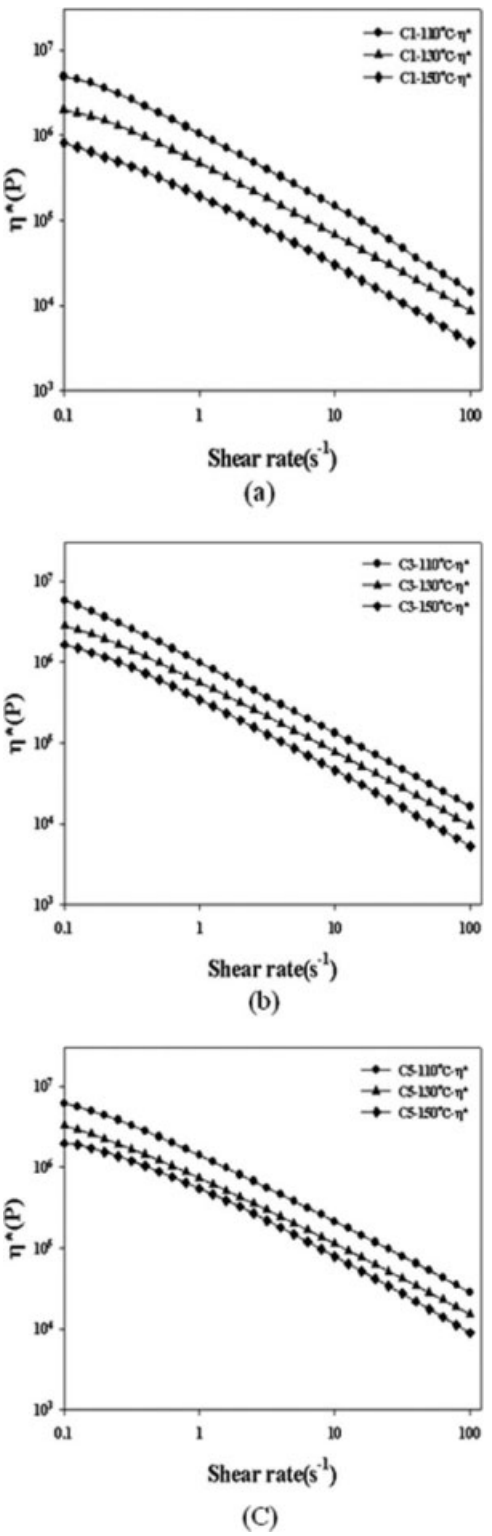

Figure 6 Complex viscosities of UHMWPE/organoclay nanocomposites at various temperatures: (a) 1 pphr, (b) 3 pphr, and (c) 5 pphr.

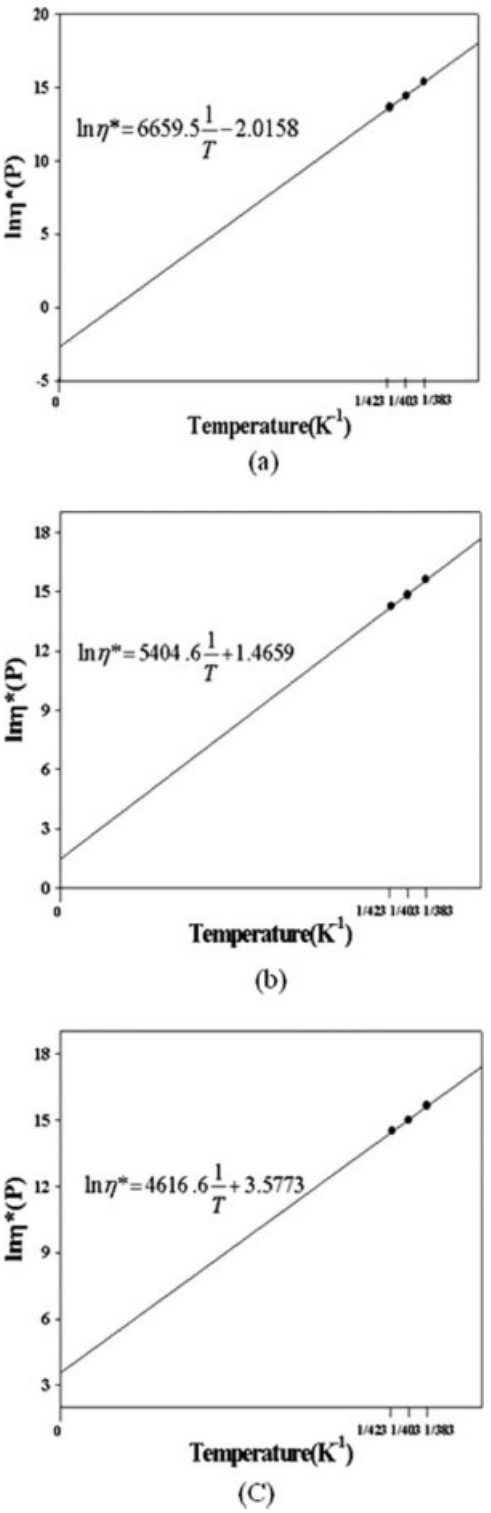

Figure 7 The Arrhenius plot of various ratio of UHMWPE/organoclay nanocomposites: (a) 1 pphr, (b) 3 pphr, and (c) 5 pphr.

$$|\eta^*| = \sqrt{(\eta')^2 + (\eta'')^2} \tag{5}$$

For UHMWPE, η'' has almost the same value with η^* in magnitude while η' is approximately one order of magnitude smaller than that of η''. This makes a contradiction to the conventional thermoplastic melts where η' is much bigger than η''. The contradiction is in part due to the low measure temperature that gives more elastic deformation than viscous deformation. However, it is mostly due to the high elasticity of the gel, which is caused by the intensive entanglements of the flexible and long UHMWPE chains. With the addition and increasing amount of organoclay, η' decreases and η'' increases, implying that mobility of UHMWPE chain is disturbed by organoclay.

Temperature-dependent viscosity is described by Arrhenius plot. Figure 7 shows the Arrhenius plot of the composite viscosities measured at three different temperatures according to

$$\eta = A \times e^{\frac{E}{RT}} \tag{6}$$

where A, E, R, and T are constant, activation energy for viscous flow, gas constant, and absolute temperature, respectively. It is seen that the viscosities of the composite gels follow Arrhenius equation. This may imply that morphology change such as main chain scission is not significant during the measurements.

It is seen that the slope of the Arrhenius plot decreases with the addition and increasing content of organoclay, indicating that the activation energy of flow and hence the dependence of viscosity on temperature decreases with increasing organoclay content.

Using the Arrhenius equation, shift factors [eq. (7)] were calculated with the reference temperature (T_0) of 130°C, and the results are given in Table III.

$$\alpha_T = \frac{\eta'}{\eta'_0} = \frac{A \times e^{\frac{E}{RT}}}{A \times e^{\frac{E}{RT_0}}} = e^{\frac{E}{R}\left(\frac{1}{T} - \frac{1}{T_0}\right)} \tag{7}$$

As expected the shift factor closes to unity as the content of organoclay increases. This implies that viscosity becomes less vulnerable to the temperature at high organoclay content.

Using the shift factors, the master curves of viscosity functions are drawn and superposed on the reference temperature in Figure 8. It is seen that the

TABLE III
Shift Factors at Various Temperatures and Organoclay Contents (Reference temperature: 130°C)

	X_c	T_m (°C)	ΔH (J/g)
UHMWPE	57.38	132.70	161.3
C0	61.94	132.61	174.1
C1	64.01	132.30	179.9
C2	65.82	131.84	185.0
C3	66.32	131.57	186.4
C5	65.29	131.18	183.5

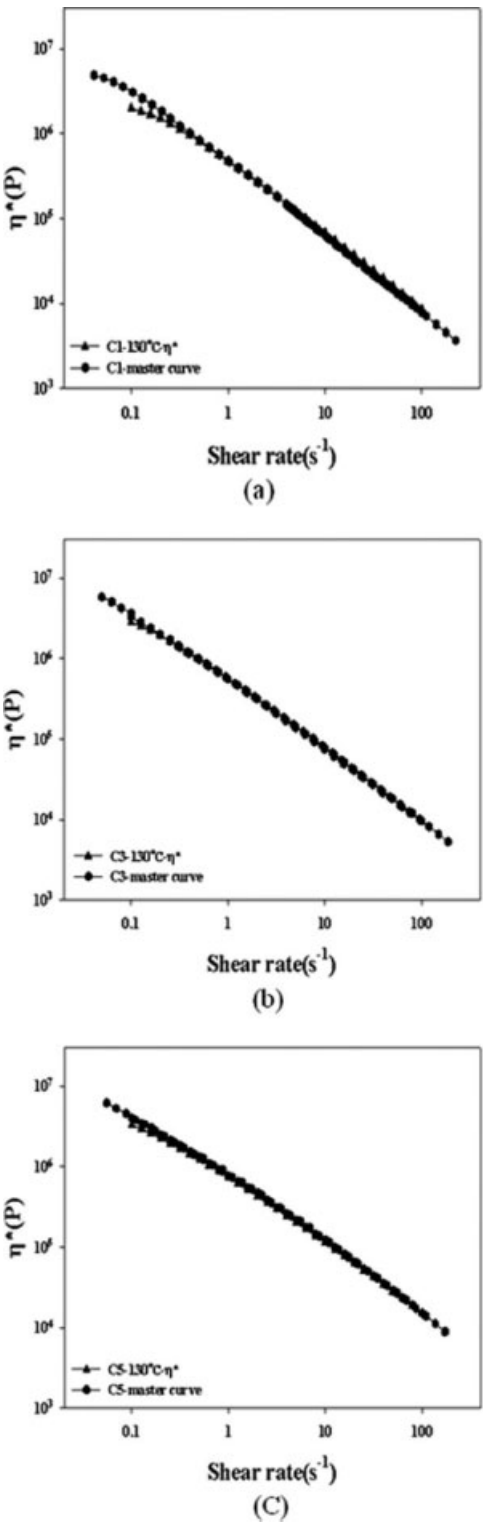

Figure 8 The master curve of various ratio of UHMWPE/organoclay nanocomposites: (a) 1 pphr, (b) 3 pphr, and (c) 5 pphr.

horizontal shifts of viscosity functions for 110 and 150°C amounting to ln α_T give fair well superposition on that of 130°C.

CONCLUSIONS

The effects of organoclay on the rheological, thermal, mechanical properties of UHMWPE/organoclay nanocomposites have been experimentally determined.

The XRD analysis clearly indicated the exfoliation of organoclay for UHMWPE/organoclay nanocomposites except the high nanoclay content (C5).

The tensile modulus and strength generally increase and elongation at break decreases with the addition and increasing amount of organoclay as compared with the virgin UHMWPE.

The addition of small amount of organoclay augmented thermal stability of the virgin UHMWPE. The crystallinity of UHMWPE has been increased with the addition and increasing amount of clay due to the nucleation effect of nanoclay. However, the effect was less pronounced with C5 due to the incomplete exfoliation.

Viscosity of UHMWPE gel increased with the addition and increasing amount of organoclay due to the increased volume of solid. Viscosity functions of the composite generally followed the power law behavior. On the other hand, temperature dependence was described by Arrhenius equation, and it became less significant with increasing clay content.

References

1. Hashmi, S. A. R.; Neogi, S.; Pandey, A.; Chand, N. Wear 2001, 247, 9.
2. Lu, S. H.; Liang, G. Z.; Zhou, Z. W.; Li, F. J Appl Polym Sci 2006, 101, 1880.
3. Huang, W.; Wang, Y.; Xia, Y. Polymer 2004, 45, 3729.
4. Prever, E. B.; Crova, M.; Costa, L.; Dallera, A.; Camino, G.; Gallinaro, P. Biomaterials 1996, 17, 873.
5. Kumar, P.; Oka, M.; Ikeuchu, K.; Shimizu, K.; Yamamuro, T.; Okumura, H.; Kotoura, Y. J Biomed Mater Res 1991, 25, 813.
6. Gai, J.; Li, H. J Appl Polym Sci 2007, 106, 3023.
7. Burroughs, B. R.; Rubash, H. E.; Estok, D.; Jasty, M.; Krevolin, J.; Muratoglu, O. K. J Biomed Mater Res B Appl Biomater 2006, 79, 268.
8. Ristolainen, N.; Vainio, U.; Paavola, S.; Torkkeli, M.; Serimaa, R.; Seppala, J. J Polym Sci B Polym Phys 2005, 43, 1892.
9. Osman, M. A.; Atallah, A. Macromol Rapid Commun 2004, 25, 1540.
10. Alexandre, M.; Dubois, P. Mater Sci Eng 2000, 28, 1.
11. Lertwimolnun, W.; Vergnes, B. Polymer 2005, 46, 3462.
12. Xi, Y.; Ishikawa, H.; Bin, Y.; Matsuo, M. Carbon 2004, 42, 1699.
13. Morley, K. S.; Webb, P. B.; Tokareva, N. V.; Krasnov, A. P.; Popov, V. K.; Zhang, J.; Roberts, C. J.; Howdle, S. M. Eur Polym J 2007, 43, 307.
14. Jung, M. H.; Kim, J. C.; Chang, J. H. Polymer (Korea) 2007, 31, 428.
15. Chang, J. H.; Jo, B. Y. J Appl Polym Sci 1996, 60, 939.
16. Chawla, K. K. Composite Materials Science and Engineering; Springer-Verlag: New York, 1987.
17. Curtin, W. A. J Am Ceram Soc 1991, 74, 2837.
18. Noh, M. H.; Jang, L. W.; Lee, D. C. J Appl Polym Sci 1999, 74, 179.
19. Chen, T. K.; Tien, Y. I.; Wei, K. H. Polymer 2000, 41, 1345.